REPORTS

NUCLEAR PHYSICS

Momentum sharing in imbalanced Fermi systems

O. Hen,[1]* M. Sargsian,[2] L. B. Weinstein,[3] E. Piasetzky,[1] H. Hakobyan,[4,5] D. W. Higinbotham,[6] M. Braverman,[1] W. K. Brooks,[4] S. Gilad,[7] K. P. Adhikari,[3] J. Arrington,[8] G. Asryan,[5] H. Avakian,[6] J. Ball,[9] N. A. Baltzell,[8] M. Battaglieri,[10] A. Beck,[1,11] S. May-Tal Beck,[1,11] I. Bedlinskiy,[12] W. Bertozzi,[7] A. Biselli,[13] V. D. Burkert,[6] T. Cao,[14] D. S. Carman,[6] A. Celentano,[10] S. Chandavar,[15] L. Colaneri,[16] P. L. Cole,[6,17,18] V. Crede,[19] A. D'Angelo,[16,20] R. De Vita,[10] A. Deur,[6] C. Djalali,[14,21] D. Doughty,[6,22] M. Dugger,[23] R. Dupre,[24] H. Egiyan,[6] A. El Alaoui,[8] L. El Fassi,[3] L. Elouadrhiri,[6] G. Fedotov,[14,25] S. Fegan,[10] T. Forest,[17] B. Garillon,[24] M. Garcon,[9] N. Gevorgyan,[5] Y. Ghandilyan,[5] G. P. Gilfoyle,[26] F. X. Girod,[6] J. T. Goetz,[15] R. W. Gothe,[14] K. A. Griffioen,[27] M. Guidal,[24] L. Guo,[2,6] K. Hafidi,[8] C. Hanretty,[28] M. Hattawy,[24] K. Hicks,[15] M. Holtrop,[29] C. E. Hyde,[3] Y. Ilieva,[14,30] D. G. Ireland,[31] B. I. Ishkanov,[25] E. L. Isupov,[25] H. Jiang,[14] H. S. Jo,[24] K. Joo,[32] D. Keller,[28] M. Khandaker,[17,33] A. Kim,[34] W. Kim,[34] F. J. Klein,[18] S. Koirala,[3] I. Korover,[1] S. E. Kuhn,[3] V. Kubarovsky,[6] P. Lenisa,[35] W. I. Levine,[36] K. Livingston,[31] M. Lowry,[6] H. Y. Lu,[14] I. J. D. MacGregor,[31] N. Markov,[32] M. Mayer,[3] B. McKinnon,[31] T. Mineeva,[32] V. Mokeev,[6,24,37] A. Movsisyan,[35] C. Munoz Camacho,[24] B. Mustapha,[8] P. Nadel-Turonski,[6] S. Niccolai,[24] G. Niculescu,[38] I. Niculescu,[38] M. Osipenko,[10] L. L. Pappalardo,[35,39] R. Paremuzyan,[5,29] K. Park,[6,34] E. Pasyuk,[6] W. Phelps,[2] S. Pisano,[40] O. Pogorelko,[12] J. W. Price,[41] S. Procureur,[9] Y. Prok,[3,28] D. Protopopescu,[31] A. J. R. Puckett,[32] D. Rimal,[2] M. Ripani,[10] B. G. Ritchie,[23] A. Rizzo,[16] G. Rosner,[31] P. Roy,[19] P. Rossi,[6] F. Sabatié,[9] D. Schott,[30] R. A. Schumacher,[36] Y. G. Sharabian,[6] G. D. Smith,[42] R. Shneor,[1] D. Sokhan,[31] S. S. Stepanyan,[34] S. Stepanyan,[6] P. Stoler,[43] S. Strauch,[14,30] V. Sytnik,[4] M. Taiuti,[44] S. Tkachenko,[28] M. Ungaro,[6] A. V. Vlassov,[12] E. Voutier,[45] N. K. Walford,[18] X. Wei,[6] M. H. Wood,[14,46] S. A. Wood,[6] N. Zachariou,[14] L. Zana,[29,42] Z. W. Zhao,[28] X. Zheng,[28] I. Zonta,[16] Jefferson Lab CLAS Collaboration†

The atomic nucleus is composed of two different kinds of fermions: protons and neutrons. If the protons and neutrons did not interact, the Pauli exclusion principle would force the majority of fermions (usually neutrons) to have a higher average momentum. Our high-energy electron-scattering measurements using ^{12}C, ^{27}Al, ^{56}Fe, and ^{208}Pb targets show that even in heavy, neutron-rich nuclei, short-range interactions between the fermions form correlated high-momentum neutron-proton pairs. Thus, in neutron-rich nuclei, protons have a greater probability than neutrons to have momentum greater than the Fermi momentum. This finding has implications ranging from nuclear few-body systems to neutron stars and may also be observable experimentally in two-spin–state, ultracold atomic gas systems.

Many-body systems composed of interacting fermions are common in nature, ranging from high-temperature superconductors and Fermi liquids to atomic nuclei, quark matter, and neutron stars. Particularly intriguing are systems that include a short-range interaction that is strong between unlike fermions and weak between the same type of fermions. Recent theoretical advances show that even though the underlying interaction can be very different, these systems share several universal features (*1*–*4*). In all of these systems, this interaction creates short-range–correlated (SRC) pairs of unlike fermions with a large relative momentum ($k_{rel} > k_F$) and a small center-of-mass momentum ($k_{tot} < k_F$), where k_F is the Fermi momentum of the system. This pushes fermions from low momenta ($k < k_F$, where k is the fermion momentum) to high momenta ($k > k_F$), creating a "high-momentum tail."

In atomic nuclei, SRC pairs have been studied using many different reactions, including pick-up, stripping, and electron and proton scattering. The results of these studies highlighted the importance of correlations in nuclei, which lead to a high-momentum tail and decreased occupancy of low-lying nuclear states (*5*–*13*).

Recent experimental studies of balanced (symmetric) interacting Fermi systems, with an equal number of fermions of the two kinds, confirmed these predictions of a high-momentum tail populated almost exclusively by pairs of unlike fermions (*8*–*11*, *14*–*16*). These experiments were carried out using very different Fermi systems: protons and neutrons in atomic nuclei and two-spin–state, ultracold atomic gases. These systems span more than 15 orders of magnitude in Fermi energy from 10^6 to 10^{-9} eV and exhibit different short-range interactions [predominantly a strong tensor interaction in the nuclear systems (*8*, *9*, *17*, *18*) and a tunable Feshbach resonance in the atomic system (*14*, *15*)]. For cold atoms, Tan (*1*–*3*) showed that the momentum density decreases as C/k^4 for large k. The scale factor, C, is known as Tan's contact and describes many properties of the system (*4*). Similar pairing of nucleons in nuclei with $k > k_F$ was also predicted in (*19*).

In this work, we extend these previous studies to imbalanced (asymmetric) nuclear systems, with unequal numbers of the different fermions. When there is no interaction, the Pauli exclusion principle pushes the majority fermions (usually neutrons) to a higher average momentum. Including a short-range interaction introduces a new universal feature: the probability for a fermion to have momentum $k > k_F$ is greater for the minority than for the majority fermions. This is because the short-range interaction populates the high-momentum

[1]Tel Aviv University, Tel Aviv 69978, Israel. [2]Florida International University, Miami, FL 33199, USA. [3]Old Dominion University, Norfolk, VA 23529, USA. [4]Universidad Técnica Federico Santa María, Casilla 110-V Valparaíso, Chile. [5]Yerevan Physics Institute, 375036 Yerevan, Armenia. [6]Thomas Jefferson National Accelerator Facility, Newport News, VA 23606, USA. [7]Massachusetts Institute of Technology, Cambridge, MA 02139, USA. [8]Argonne National Laboratory, Argonne, IL 60439, USA. [9]Commissariat à l'Energie Atomique et aux Energies Alternatives, Centre de Saclay, Irfu/Service de Physique Nucléaire, 91191 Gif-sur-Yvette, France. [10]Istituto Nazionale di Fisica Nucleare (INFN), Sezione di Genova, 16146 Genova, Italy. [11]Nuclear Research Center Negev, P.O. Box 9001, Beer-Sheva 84190, Israel. [12]Institute of Theoretical and Experimental Physics, Moscow, 117259, Russia. [13]Fairfield University, Fairfield, CT 06824, USA. [14]University of South Carolina, Columbia, SC 29208, USA. [15]Ohio University, Athens, OH 45701, USA. [16]INFN, Sezione di Roma Tor Vergata, 00133 Rome, Italy. [17]Idaho State University, Pocatello, ID 83209, USA. [18]Catholic University of America, Washington, DC 20064, USA. [19]Florida State University, Tallahassee, FL 32306, USA. [20]Università di Roma Tor Vergata, 00133 Rome, Italy. [21]University of Iowa, Iowa City, IA 52242, USA. [22]Christopher Newport University, Newport News, VA 23606, USA. [23]Arizona State University, Tempe, AZ 85287-1504, USA. [24]Institut de Physique Nucléaire ORSAY, Orsay, France. [25]Skobeltsyn Institute of Nuclear Physics, Lomonosov, Russia. [26]University of Richmond, Richmond, VA 23173, USA. [27]College of William and Mary, Williamsburg, VA 23187-8795, USA. [28]University of Virginia, Charlottesville, VA 22901, USA. [29]University of New Hampshire, Durham, NH 03824-3568, USA. [30]The George Washington University, Washington, DC 20052, USA. [31]University of Glasgow, Glasgow G12 8QQ, UK. [32]University of Connecticut, Storrs, CT 06269, USA. [33]Norfolk State University, Norfolk, VA 23504, USA. [34]Kyungpook National University, Daegu 702-701, Republic of Korea. [35]INFN, Sezione di Ferrara, 44100 Ferrara, Italy. [36]Carnegie Mellon University, Pittsburgh, PA 15213, USA. [37]Moscow State University, Moscow, 119234, Russia. [38]James Madison University, Harrisonburg, VA 22807, USA. [39]Universitá di Ferrara, 44122 Ferrara, Italy. [40]INFN, Laboratori Nazionali di Frascati, 00044 Frascati, Italy. [41]California State University, Dominguez Hills, Carson, CA 90747, USA. [42]Edinburgh University, Edinburgh EH9 3JZ, UK. [43]Rensselaer Polytechnic Institute, Troy, NY 12180-3590, USA. [44]Università di Genova, 16146 Genova, Italy. [45]Laboratoire de Physique Subatomique et de Cosmologie, Universite Joseph Fourier, CNRS/IN2P3, Institut National Polytechnique, Grenoble, France. [46]Canisius College, Buffalo, NY 14208, USA.

***Corresponding author. E-mail: or.chen@mail.huji.ac.il** †The collaboration on this paper consists of all listed authors. There are no additional collaborators.

tail with equal numbers of majority and minority fermions, thereby leaving a larger fraction of majority fermions in low-momentum states ($k < k_F$) (see Fig. 1). In neutron-rich nuclei, this increases the average proton momentum and may even result in protons having higher average momentum than neutrons, inverting the momentum sharing in imbalanced nuclei from that in noninteracting systems. Theoretically, this can happen because of the tensor part of the nucleon-nucleon interaction, which creates predominantly spin-1, isospin-0 neutron-proton (np) SRC pairs (*17*, *18*).

Here we identify SRC pairs in the high-momentum tail of nuclei heavier than carbon with more neutrons (N) than protons (Z) (i.e., $N > Z$). The data show the universal nature of SRC pairs, which even in lead (N/Z = 126/82) are still predominantly np pairs. This np-pair dominance causes a greater fraction of protons than neutrons to have high momentum in neutron-rich nuclei.

The data presented here were collected in 2004 in Hall B of the Thomas Jefferson National Accelerator Facility using a 5.014-GeV electron beam incident on ^{12}C, ^{27}Al, ^{56}Fe, and ^{208}Pb targets. We measured electron-induced two-proton knockout reactions (Fig. 2). The CEBAF Large Acceptance Spectrometer (CLAS) (*20*) was used to detect the scattered electron and emitted protons. CLAS uses a toroidal magnetic field and six independent sets of drift chambers, time-of-flight scintillation counters, Cerenkov counters, and electromagnetic calorimeters for charged-particle identification and trajectory reconstruction (Fig. 2) (*16*).

We selected events in which the electron interacts with a single fast proton from an SRC pair in the nucleus (*9*, *16*) by requiring a large four-momentum transfer $Q^2 = \vec{q}^{\,2} - (\omega/c)^2 > 1.5$ GeV$^2/c^2$ [where $\vec{q}$ and ω are the three-momentum and energy, respectively, transferred to the nucleus and c is the speed of light] and Bjorken scaling parameter $x_B = Q^2/(2m_N \cdot \omega) > 1.2$ (where m_N is the nucleon mass). To ensure selection of events in which the knocked-out proton belonged to an SRC pair, we further required missing momentum $300 < |\vec{p}_{miss}| < 600$ MeV/c, where $\vec{p}_{miss} = \vec{p}_p - \vec{q}$ with $\vec{p}_p$ the measured proton momentum. We suppressed contributions from inelastic excitations of the struck nucleon by limiting the reconstructed missing mass of the two-nucleon system $m_{miss} < 1.1$ GeV/c^2. In each event, the leading proton that absorbed the transferred momentum was identified by requiring that its momentum $\vec{p}_p$ is within 25° of $\vec{q}$ and that $|\vec{p}_p|/|\vec{q}| \geq 0.6$ (*16*, *21*).

When a second proton was detected with momentum greater than 350 MeV/c, it was emitted almost diametrically opposite to $\vec{p}_{miss}$ (see fig. S19). The observed backward-peaked angular distributions are very similar for all four measured

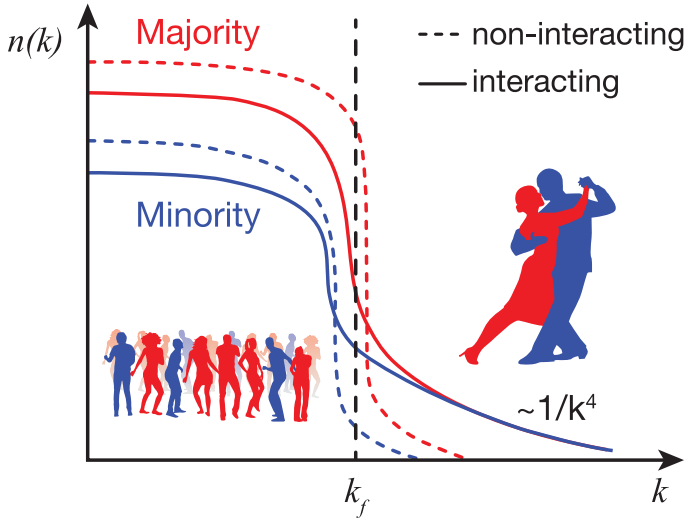

Fig. 1. Schematic representation of the momentum distribution, $n(k)$, of two-component imbalanced Fermi systems. Red and blue dashed lines show the noninteracting system, whereas the solid lines show the effect of including a short-range interaction between different fermions. Such interactions create a high-momentum tail ($k > k_F$, where k_F is the Fermi momentum of the system). This is analogous to a dance party with a majority of girls, where boy-girl interactions will make the average boy dance more than the average girl.

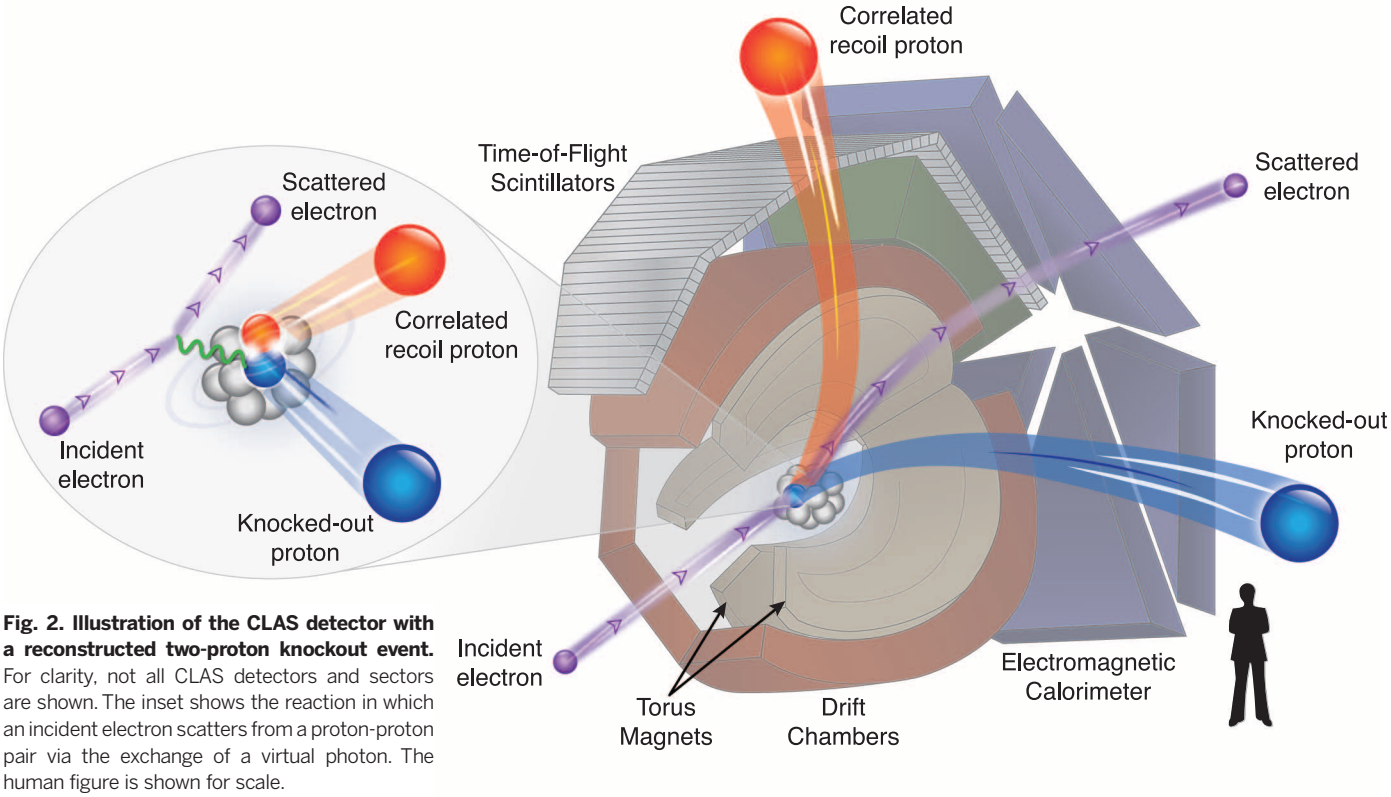

Fig. 2. Illustration of the CLAS detector with a reconstructed two-proton knockout event. For clarity, not all CLAS detectors and sectors are shown. The inset shows the reaction in which an incident electron scatters from a proton-proton pair via the exchange of a virtual photon. The human figure is shown for scale.

nuclei. This backward peak is a strong signature of SRC pairs, indicating that the two emitted protons were largely back-to-back in the initial state, having a large relative momentum and a small center-of-mass momentum (*8*, *9*). This is a direct observation of proton-proton (pp) SRC pairs in a nucleus heavier than ^{12}C.

Electron scattering from high–missing-momentum protons is dominated by scattering from protons in SRC pairs (*9*). The measured single-proton knockout ($e,e'p$) cross section (where e denotes the incoming electron, e' the measured scattered electron, and p the measured knocked-out proton) is sensitive to the number of pp and np SRC pairs in the nucleus, whereas the two-proton knockout ($e,e'pp$) cross section is only sensitive to the number of pp-SRC pairs. Very few of the single-proton knockout events also contained a second proton; therefore, there are very few pp pairs, and the knocked-out protons predominantly originated from np pairs.

To quantify this, we extracted the $[A(e,e'pp)/A(e,e'p)]/[^{12}C(e,e'pp)/^{12}C(e,e'p)]$ cross-section double ratio for nucleus A relative to ^{12}C. The double ratio is sensitive to the ratio of np-to-pp SRC pairs in the two nuclei (*16*). Previous measurements have shown that in ^{12}C nearly every high-momentum proton ($k > 300$ MeV/$c > k_F$) has a correlated partner nucleon, with np pairs outnumbering pp pairs by a factor of ~20 (*8*, *9*).

To estimate the effects of final-state interactions (reinteraction of the outgoing nucleons in the nucleus), we calculated attenuation factors for the outgoing protons and the probability of the electron scattering from a neutron in an np pair, followed by a neutron-proton single-charge exchange (SCX) reaction leading to two outgoing protons. These correction factors are calculated as in (*9*) using the Glauber approximation (*22*) with effective cross sections that reproduce previously measured proton transparencies (*23*), and using the measured SCX cross section of (*24*). We extracted the cross-section ratios and deduced the relative pair fractions from the measured yields following (*21*); see (*16*) for details.

Figure 3 shows the extracted fractions of np and pp SRC pairs from the sum of pp and np pairs in nuclei, including all statistical, systematic, and model uncertainties. Our measurements are not sensitive to neutron-neutron SRC pairs. However, by a simple combinatoric argument, even in ^{208}Pb these would be only $(N/Z)^2 \sim 2$ times the number of pp pairs. Thus, np-SRC pairs dominate in all measured nuclei, including neutron-rich imbalanced ones.

The observed dominance of np-over-pp pairs implies that even in heavy nuclei, SRC pairs are dominantly in a spin-triplet state (spin 1, isospin 0), a consequence of the tensor part of the nucleon-nucleon interaction (*17*, *18*). It also implies that there are as many high-momentum protons as neutrons (Fig. 1) so that the fraction of protons above the Fermi momentum is greater than that of neutrons in neutron-rich nuclei (*25*).

In light imbalanced nuclei ($A \leq 12$), variational Monte Carlo calculations (*26*) show that this results in a greater average momentum for the minority component (see table S1). The minority component can also have a greater average momentum in heavy nuclei if the Fermi momenta of protons and neutrons are not too dissimilar. For heavy nuclei, an np-dominance toy model that quantitatively describes the features of the momentum distribution shown in Fig. 1 shows that in imbalanced nuclei, the average proton kinetic energy is greater than that of the neutron, up to ~20% in ^{208}Pb (*16*).

The observed np-dominance of SRC pairs in heavy imbalanced nuclei may have wide-ranging implications. Neutrino scattering from two nucleon currents and SRC pairs is important for the analysis of neutrino-nucleus reactions, which are used to study the nature of the electro-weak interaction (*27*–*29*). In particle physics, the distribution of quarks in these high-momentum nucleons in SRC pairs might be modified from that of free nucleons (*30*, *31*). Because each proton has a greater probability to be in a SRC pair than a neutron and the proton has two u quarks for each d quark, the u-quark distribution modification could be greater than that of the d quarks (*19*, *30*). This could explain the difference between the weak mixing angle measured on an iron target by the NuTeV experiment and that of the Standard Model of particle physics (*32*–*34*).

In astrophysics, the nuclear symmetry energy is important for various systems, including neutron stars, the neutronization of matter in core-collapse supernovae, and r-process nucleosynthesis (*35*). The decomposition of the symmetry energy at saturation density ($\rho_0 \approx 0.17$ fm^{-3}, the maximum density of normal nuclei) into its kinetic and potential parts and its value at supranuclear densities ($\rho > \rho_0$) are not well constrained, largely because of the uncertainties in the tensor component of the nucleon-nucleon interaction (*36*–*39*). Although at supranuclear densities other effects are relevant, the inclusion of high-momentum tails, dominated by tensor-force–induced np-SRC pairs, can notably soften the nuclear symmetry energy (*36*–*39*). Our measurements of np-SRC pair dominance in heavy imbalanced nuclei can help constrain the nuclear aspects of these calculations at saturation density.

Based on our results in the nuclear system, we suggest extending the previous measurements of Tan's contact in balanced ultracold atomic gases to imbalanced systems in which the number of atoms in the two spin states is different. The large experimental flexibility of these systems will allow observing dependence of the momentum-sharing inversion on the asymmetry, density, and strength of the short-range interaction.

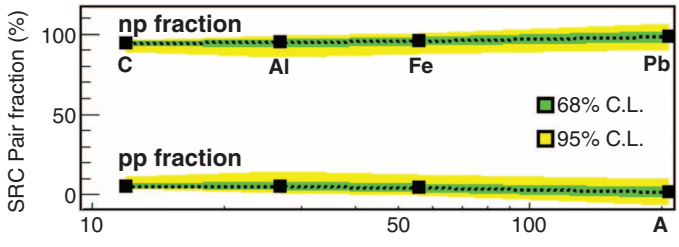

Fig. 3. The extracted fractions of np (top) and pp (bottom) SRC pairs from the sum of pp and np pairs in nuclei. The green and yellow bands reflect 68 and 95% confidence levels (CLs), respectively (*9*). np-SRC pairs dominate over pp-SRC pairs in all measured nuclei.

REFERENCES AND NOTES

1. S. Tan, *Ann. Phys.* **323**, 2952–2970 (2008).
2. S. Tan, *Ann. Phys.* **323**, 2971–2986 (2008).
3. S. Tan, *Ann. Phys.* **323**, 2987–2990 (2008).
4. E. Braaten, in *Lecture Notes in Physics* (Springer, Berlin, 2012), vol. 836, p. 193.
5. L. Lapikás, *Nucl. Phys. A.* **553**, 297–308 (1993).
6. K. I. Blomqvist *et al.*, *Phys. Lett. B* **421**, 71–78 (1998).
7. R. Starink *et al.*, *Phys. Lett. B* **474**, 33–40 (2000).
8. E. Piasetzky, M. Sargsian, L. Frankfurt, M. Strikman, J. W. Watson, *Phys. Rev. Lett.* **97**, 162504 (2006).
9. R. Subedi *et al.*, *Science* **320**, 1476–1478 (2008).
10. K. Sh. Egiyan *et al.*, *Phys. Rev. Lett.* **96**, 082501 (2006).
11. N. Fomin *et al.*, *Phys. Rev. Lett.* **108**, 092502 (2012).
12. V. R. Pandharipande, I. Sick, P. K. A. deWitt Huberts, *Rev. Mod. Phys.* **69**, 981–991 (1997).
13. J. Arrington, D. W. Higinbotham, G. Rosner, M. Sargsian, *Prog. Part. Nucl. Phys.* **67**, 898–938 (2012).
14. J. T. Stewart, J. P. Gaebler, T. E. Drake, D. S. Jin, *Phys. Rev. Lett.* **104**, 235301 (2010).
15. E. D. Kuhnle *et al.*, *Phys. Rev. Lett.* **105**, 070402 (2010).
16. Materials and methods are available as supplementary materials on *Science* Online.
17. R. Schiavilla, R. B. Wiringa, S. C. Pieper, J. Carlson, *Phys. Rev. Lett.* **98**, 132501 (2007).
18. M. M. Sargsian, T. V. Abrahamyan, M. I. Strikman, L. L. Frankfurt, *Phys. Rev. C* **71**, 044615 (2005).
19. L. Frankfurt, M. Strikman, *Phys. Rep.* **160**, 235–427 (1988).
20. B. A. Mecking *et al.*, *Nucl. Inst. Meth. A* **503**, 513–553 (2003).
21. O. Hen *et al.*, *Phys. Lett. B* **722**, 63–68 (2013).
22. I. Mardor, Y. Mardor, E. Piasetsky, J. Alster, M. M. Sargsyan, *Phys. Rev. C* **46**, 761–767 (1992).
23. D. Dutta, K. Hafidi, M. Strikman, *Prog. Part. Nucl. Phys.* **69**, 1–27 (2013).
24. J. L. Friedes, H. Palevsky, R. Stearns, R. Sutter, *Phys. Rev. Lett.* **15**, 38–41 (1965).
25. M. M. Sargsian, *Phys. Rev. C* **89**, 034305 (2014).
26. R. B. Wiringa, R. Schiavilla, S. C. Pieper, J. Carlson, *Phys. Rev. C* **89**, 024305 (2014).
27. L. Fields *et al.*, *Phys. Rev. Lett.* **111**, 022501 (2013).
28. G. A. Fiorentini *et al.*, *Phys. Rev. Lett.* **111**, 022502 (2013).
29. Neutrino-Nucleus Interactions for Current and Next Generation Neutrino Oscillation Experiments, Institute for Nuclear Theory (INT) workshop INT-13-54W, University of Washington, Seattle, WA, 3 to 13 December 2013.
30. O. Hen, D. W. Higinbotham, G. A. Miller, E. Piasetzky, L. B. Weinstein, *Int. J. Mod. Phys. E* **22**, 133017 (2013).
31. L. B. Weinstein *et al.*, *Phys. Rev. Lett.* **106**, 052301 (2011).
32. G. P. Zeller *et al.*, *Phys. Rev. Lett.* **88**, 091802 (2002).
33. G. P. Zeller *et al.*, *Phys. Rev. Lett.* **90**, 239902 (2003).
34. I. C. Cloët, W. Bentz, A. W. Thomas, *Phys. Rev. Lett.* **102**, 252301 (2009).
35. J. M. Lattimer, Y. Lim, *Astrophys. J.* **771**, 51 (2013).
36. A. Carbone, A. Polls, A. Rios, *Europhys. Lett.* **97**, 22001 (2012).
37. I. Vidana, A. Polls, C. Providencia, *Phys. Rev. C* **84**, 062801(R) (2011).
38. C. Xu, A. Li, B. A. Li, *J. Phys. Conf. Ser.* **420**, 012090 (2013).
39. B.-A. Li, L.-W. Chen, C. M. Ko, *Phys. Rep.* **464**, 113–281 (2008).

ACKNOWLEDGMENTS

This work was supported by the U.S. Department of Energy (DOE) and the National Science Foundation, the Israel Science Foundation, the Chilean Comisión Nacional de Investigación Científica y Tecnológica, the French Centre National de la

Recherche Scientifique and Commissariat a l'Energie Atomique, the French-American Cultural Exchange, the Italian Istituto Nazionale di Fisica Nucleare, the National Research Foundation of Korea, and the UK's Science and Technology Facilities Council. Jefferson Science Associates operates the Thomas Jefferson National Accelerator Facility for the DOE, Office of Science, Office of Nuclear Physics under contract DE-AC05-06OR23177. The raw data from this experiment are archived in Jefferson Lab's mass storage silo.

SUPPLEMENTARY MATERIALS

www.sciencemag.org/content/346/6209/614/suppl/DC1
Materials and Methods
Figs. S1 to S30
Tables S1 to S8
References (*40*–*51*)

2 June 2014; accepted 2 October 2014
Published online 16 October 2014;
10.1126/science.1256785

VOLCANOLOGY

A large magmatic sill complex beneath the Toba caldera

K. Jaxybulatov,[1,2,3] N. M. Shapiro,[3]* I. Koulakov,[1,2] A. Mordret,[3] M. Landès,[3] C. Sens-Schönfelder[4]

An understanding of the formation of large magmatic reservoirs is a key issue for the evaluation of possible strong volcanic eruptions in the future. We estimated the size and level of maturity of one of the largest volcanic reservoirs, based on radial seismic anisotropy. We used ambient-noise seismic tomography below the Toba caldera (in northern Sumatra) to observe the anisotropy that we interpret as the expression of a fine-scale layering caused by the presence of many partially molten sills in the crust below 7 kilometers. This result demonstrates that the magmatic reservoirs of present (non-eroded) supervolcanoes can be formed as large sill complexes and supports the concept of the long-term incremental evolution of magma bodies that lead to the largest volcanic eruptions.

The size and type of a volcanic eruption depend on the processes that occur in the magmatic reservoirs in Earth's crust. In particular, the largest eruptions require the building of extended pools of viscous gas-rich magma within the crust (*1*–*3*). In the present study, we investigated the magmatic system that produced one of the strongest eruptions in the Quaternary: the Toba event that occurred 74,000 years ago in northern Sumatra, Indonesia (Fig. 1), and emitted at least 2800 cubic kilometers of volcanic material (*4*). This catastrophe is believed to have affected the global climate and to have had a strong impact on the biosphere (*4*, *5*). The event was preceded during the previous 2 million years by at least four other eruptions in nearby locations that had volcano explosivity indices above 7 (*4*). The generation of this exceptional sequence of eruptions could be possible with the existence of a very large magma reservoir in the crust that formed over a long period of time (>1 million years) (*6*). Considering the relatively short period of time that has passed since the main Toba event, the structures that were responsible for the formation and functioning of this reservoir are expected to be well preserved in the Sumatra crust to date. Combined with previous geophysical investigations, the new data presented here provide us with information about the structure of the Toba volcano-magmatic complex and help us to better understand the internal structure and ascent mechanism of large magma volumes through the crust before their super-eruptions.

Geological observations of eroded and exposed past volcanoes and geodynamic models indicate that volcano-magmatic reservoirs evolve over long periods of time and grow in small increments, with the formation of dykes or sills (*2*, *3*, *7*–*9*). However, the exact mechanisms involved in the ascent and emplacement of the magma in the crust beneath active volcanoes are not yet completely understood, mainly because of the lack of detailed information about the structures of volcano-magmatic complexes below volcanoes in their most productive phase. Large-scale images of zones affected by melts can be obtained with magneto-telluric methods (*10*) and with seismic tomography (*11*). Some signatures of large crustal intrusions can also be detected by receiver functions (*12*). However, the individual dykes or sills within magmatic complexes that have metric or decametric thicknesses (*7*) cannot be deduced from geophysical imaging alone, and as layered intrusions, their interpretation requires additional geological information (*13*).

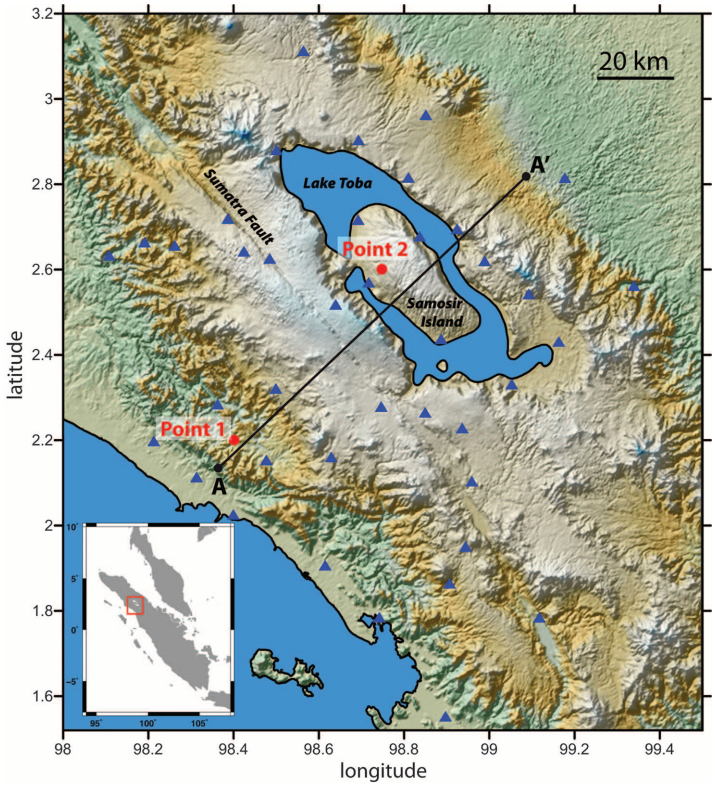

Fig. 1. Topographic map of the Lake Toba region. Blue triangles, locations of the seismic stations; black line, profile for cross sections shown in Fig. 3; red circles, locations where 1D inversion is illustrated in figs. S6 and S8. (Inset) Location of the Lake Toba region within northern Sumatra.

[1]Trofimuk Institute of Petroleum Geology and Geophysics, Siberian Branch of Russian Academy of Sciences, Prospekt Koptyuga, 3, Novosibirsk 630090, Russia. [2]Novosibirsk State University, 2, Pirogova Street, Novosibirsk 630090, Russia. [3]Institut de Physique du Globe de Paris, Sorbonne Paris Cité, CNRS (UMR 7154), 1 rue Jussieu, 75238 Paris, Cedex 5, France. [4]GFZ German Research Centre for Geosciences, Telegrafenberg 14473 Potsdam, Germany.
*Corresponding author. E-mail: nshapiro@ipgp.fr

Science

Momentum sharing in imbalanced Fermi systems

O. Hen, M. Sargsian, L. B. Weinstein, E. Piasetzky, H. Hakobyan, D. W. Higinbotham, M. Braverman, W. K. Brooks, S. Gilad, K. P. Adhikari, J. Arrington, G. Asryan, H. Avakian, J. Ball, N. A. Baltzell, M. Battaglieri, A. Beck, S. May-Tal Beck, I. Bedlinskiy, W. Bertozzi, A. Biselli, V. D. Burkert, T. Cao, D. S. Carman, A. Celentano, S. Chandavar, L. Colaneri, P. L. Cole, V. Crede, A. D'Angelo, R. De Vita, A. Deur, C. Djalali, D. Doughty, M. Dugger, R. Dupre, H. Egiyan, A. El Alaoui, L. El Fassi, L. Elouadrhiri, G. Fedotov, S. Fegan, T. Forest, B. Garillon, M. Garcon, N. Gevorgyan, Y. Ghandilyan, G. P. Gilfoyle, F. X. Girod, J. T. Goetz, R. W. Gothe, K. A. Griffioen, M. Guidal, L. Guo, K. Hafidi, C. Hanretty, M. Hattawy, K. Hicks, M. Holtrop, C. E. Hyde, Y. Ilieva, D. G. Ireland, B. I. Ishkanov, E. L. Isupov, H. Jiang, H. S. Jo, K. Joo, D. Keller, M. Khandaker, A. Kim, W. Kim, F. J. Klein, S. Koirala, I. Korover, S. E. Kuhn, V. Kubarovsky, P. Lenisa, W. I. Levine, K. Livingston, M. Lowry, H. Y. Lu, I. J. D. MacGregor, N. Markov, M. Mayer, B. McKinnon, T. Mineeva, V. Mokeev, A. Movsisyan, C. Munoz Camacho, B. Mustapha, P. Nadel-Turonski, S. Niccolai, G. Niculescu, I. Niculescu, M. Osipenko, L. L. Pappalardo, R. Paremuzyan, K. Park, E. Pasyuk, W. Phelps, S. Pisano, O. Pogorelko, J. W. Price, S. Procureur, Y. Prok, D. Protopopescu, A. J. R. Puckett, D. Rimal, M. Ripani, B. G. Ritchie, A. Rizzo, G. Rosner, P. Roy, P. Rossi, F. Sabatié, D. Schott, R. A. Schumacher, Y. G. Sharabian, G. D. Smith, R. Shneor, D. Sokhan, S. S. Stepanyan, S. Stepanyan, P. Stoler, S. Strauch, V. Sytnik, M. Taiuti, S. Tkachenko, M. Ungaro, A. V. Vlassov, E. Voutier, N. K. Walford, X. Wei, M. H. Wood, S. A. Wood, N. Zachariou, L. Zana, Z. W. Zhao, X. Zheng, I. Zonta and Jefferson Lab CLAS Collaboration

Science **346** (6209), 614-617.
DOI: 10.1126/science.1256785originally published online October 16, 2014

Scattering electrons off nuclear targets

Atomic nuclei consist of fermions—protons and neutrons—bound together by interactions. Because two identical fermions cannot occupy the same quantum state, both protons and neutrons have a broad range of momenta inside the nucleus. Hen *et al.* scattered electrons off nuclei of varying sizes to study the distribution of the protons' and neutrons' momenta. Protons formed high-momentum pairs with neutrons much more frequently than with other protons. Thus, surprisingly, the average momentum of a neutron was lower than that of a proton, even in nuclei with a larger number of neutrons than protons.

Science, this issue p. 614